

## Computational Study of Shock Wave Propagation and Reflection in a Micro Shock Tube

Arun Kumar R<sup>1</sup>, Heuy Dong Kim<sup>1\*</sup>, and Toshiaki Setoguchi<sup>2</sup>

<sup>1\*</sup>Author for correspondence

Department of Mechanical Engineering,  
 Andong National University,  
 Andong, South Korea

E-mail: kimhd@andong.ac.kr<sup>1\*</sup>, kumar@anuis.andong.ac.kr<sup>1</sup>

<sup>2</sup>Department of Mechanical Engineering, Saga University, Saga, Japan

### ABSTRACT

Micro shock tubes are miniature devices used for a variety of application in small scale devices likes MEMS equipments. The inherent low flow dimensions combined with low operating pressure makes these devices to behave differently compared to macro shock tubes. In the present study a CFD method was employed to study the shock propagation and reflection inside a micro shock tube. The shock propagation under rarefied conditions due to the low pressure prevailing in the system was studied, in detail. Navier-Stokes equation together with Maxwell's slip equations were used to simulate the rarefied flow. In these devices, boundary layer effects become a significant parameter in controlling the shock movement and strength owing to its small flow diameter. This paper focuses on giving detail explanation for the disparities in flow physics and its effect on shock movement for micro shock tube under different low pressure and diameter conditions. The results show a greater loss in the shock strength as the diameter or pressure decreases and hence shock waves get attenuated.

### INTRODUCTION

Last decade has seen much advancement in the field of micro scale devices and its implementation in various fields like microelectronic devices, micro combustion equipments, drug delivery systems etc. The quest for replacing the macro components with micro devices to reduce the system weight, structural complexity etc is one of the major challenges for today's engineering and scientific community. One such device which has a wide potential in the field of aerospace, combustion technology and drug delivery systems is a micro shock tube. The physical features of a micro shock tube are same as compared to macro shock tube except its low flow diameter. Most of these small scale devices operate at very low pressure and these causes the molecular effects to become predominant. The dilute gas at these situations causes the wall attached fluid to slip rather attaching to wall. The near wall fluid temperature also shows a jump in its value compared to

the wall. Based on the Knudsen Number, which is the ratio of molecular mean free path to flow diameter, the mathematical simulations of flow physics can be done using N-S equations, N-S equations with slip wall or molecular dynamics, which are in general manifested in such kind of rarefied gas flow theories. The above mentioned effects make the micro shock tube to show different shock characteristics compared to its macro counterpart.

One among the pioneer to start the study on micro shock tube was Duff [1]. He conducted experimental study on small shock tube of 28.6 mm diameter under low pressure condition. He noticed that shock strength get diminished quickly for shock tube with small diameters and he concluded that this attenuation effect is due to the boundary layer effects on the flow. A numerical model to account for this boundary layer effect was developed by Mirels [2]. Later studies conducted by Brouillette [3] on micro shock tube with different low driven section pressure revealed that the shock attenuation is more drastic as the pressure decreases. He also proposed a scaling factor for the generation and propagation of shock wave. Numerical simulations on shock propagation inside a micro shock tube of 5 mm diameter under rarefied conditions were carried out by Zeitoun [4, 5]. Later Fitchman [6] proposed a new analytical model to describe the slip velocity effects. Amit [7] studied the effect of gas flow in micro channels with sudden expansion and contraction. The effect of surface roughness on micro tube heat transfer was studied by Giulio [8].

Very few studies were done in the past to understand the influence of rarefaction effects on shock propagation. Also there are hardly few papers describing the shock reflection characteristics under slip conditions. Even though the flow dimension is low the high speed moving shock wave produce small scale eddies and a transition or weak turbulent flow can be expected in a micro shock tube. Through this paper we tried to produce much more detailed information on the shock wave flow physics for a micro shock tube and shock attenuation dependency on tube diameter and initial pressure.

## NOMENCLATURE

$a$	[m/s]	Sound speed
$a_t$	[-]	Thermal accommodation coefficient
$a_v$	[-]	Momentum accommodation coefficient
$k_B$	[-]	Boltzmann Number
$M$	[-]	Mach Number
$P$	[Pa]	Pressure
$T$	[K]	Temperature
$U$	[m/s]	Velocity
$x$	[m]	Cartesian axis direction

### Special characters

$\gamma$	[-]	Ratio of specific heats
$\delta$	[m]	First layer height
$\lambda$	[-]	Molecular mean free path
$\sigma$	[angstrom]	L-J characteristics length

### Subscripts

$w$	Wall quantities
$g$	Gas quantities
$c$	Cell centre quantities
$s$	Shock wave

## COMPUTATIONAL MODEL AND INITIAL CONDITIONS

For the present study a two dimensional axi-symmetric model of micro shock tube with various diameters were considered. A micro shock tube consists of a driver and driven section separated by a diaphragm with former having a higher pressure than the latter. When the diaphragm breaks highly unsteady flow evolves and this leads to the production of shock waves which moves into the driven section increasing the pressure there. A schematic diagram of the shock tube is shown in Fig. 1.

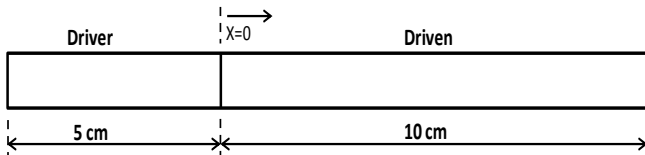


**Figure 1** Schematic diagram of computational domain

The computational domain was discretized using structured quad elements. A fine layer of mesh was created near to the wall to capture the boundary layer effects. The effect of initial pressure and slip conditions were studied on a micro shock tube of 2mm diameter. The details regarding the initial condition are shown in Table.1.

Cases	$P_4/P_1$	$P_1$	Diameter	Wall Conditions
A	15	500 Pa	2 mm	No Slip
B	15	50 Pa	2 mm	No Slip
C	15	50 Pa	2 mm	Slip

**Table 1** Initial condition to study the pressure dependency and slip effects on shock propagation

Later investigation of diameter effect on shock characteristics was studied using three different tube diameters of 2mm, 1mm and 0.5mm respectively which are shown in Table.2.

Cases	$P_4/P_1$	$P_1$	Diameter	Wall Conditions
1	15	50 Pa	2 mm	Slip
2	15	50 Pa	1 mm	Slip
3	15	50 Pa	0.5 mm	Slip

**Table 2** Initial conditions to study the diameter dependency on shock propagation in micro shock tubes

## NUMERICAL METHOD

The flow physics was mathematically modeled using unsteady Reynolds Averaged Navier-Stokes equations. The governing equations in the cartesian form can be written as,

Continuity

$$\frac{\partial \rho}{\partial t} + \frac{\partial}{\partial x_i} (\rho u_i) = 0 \quad (1)$$

Momentum

$$\frac{\partial}{\partial t} (\rho u_i) + \frac{\partial}{\partial x_i} (\rho u_i u_j) = -\frac{\partial p}{\partial x_i} + \frac{\partial}{\partial x_j} \left[ \mu \left( \frac{\partial u_i}{\partial x_j} + \frac{\partial u_j}{\partial x_i} - \frac{2}{3} \delta_{ij} \frac{\partial u_k}{\partial x_k} \right) \right] + \frac{\partial}{\partial x_j} (-\rho u_i u_j') \quad (2)$$

Energy

$$\frac{\partial \rho E}{\partial t} + \frac{\partial}{\partial x_i} [u_i (\rho E + p)] = \frac{\delta}{\partial x_i} \left[ \left( \alpha + \frac{C_p \mu_t}{P_{rt}} \right) \frac{\partial T}{\partial x_i} + u_j (\tau_{ij})_{eff} \right] \quad (3)$$

$\tau_{eff}$  is the shear stress tensor which is modeled as,

$$\tau_{ij} = \mu_{eff} \left( \frac{\partial u_j}{\partial x_i} + \frac{\partial u_i}{\partial x_j} \right) - \frac{2}{3} \mu_{eff} \frac{\partial u_k}{\partial x_k} \delta_{ij} \quad (4)$$

The shock disturbance produces flow fluctuations to the downstream boundary layer which makes the flow either transitional or turbulent, even though the diameter is very small. SST k- $\omega$  model was used to predict the turbulent eddies. In this model the turbulent viscosity is calculated by solving the transport equation for turbulent kinetic energy (k) and the specific dissipation rate ( $\omega$ ) as shown in the below equation.

$$\frac{\partial \rho k}{\partial t} + \frac{\partial}{\partial x_i} (\rho k u_i) = \frac{\delta}{\partial x_j} \left( \Gamma_k \frac{\partial k}{\partial x_j} \right) + G_k - Y_k \quad (5)$$

$$\frac{\partial \rho \omega}{\partial t} + \frac{\partial}{\partial x_i} (\rho \omega u_i) = \frac{\delta}{\partial x_j} \left( \Gamma_\omega \frac{\partial \omega}{\partial x_j} \right) + G_\omega - Y_\omega + D_\omega \quad (6)$$

At the beginning of the analysis the driver section was assumed to be filled with helium and driven section with air. The mass fraction distribution of different species involved was modeled using species transport equations. Ideal gas behavior was considered for all the species and viscosity variation with respect to temperature was modeled using Sutherland viscosity model. The flux component of the governing equation was discretized using AUSM scheme. A second order implicit scheme was used for the temporal discretization. The extrapolation of cell centre values to the face centres was done using third order MUSCL schemes. The governing flow equations were solved in a coupled manner using commercial solver, Fluent. To account for the rarefaction effects which happen at low pressure Maxwell's slip velocity and temperature jump equations [9], as shown below, were employed. User defined functions [10] were used to input these equations to the solver and subsequent to each flow iteration the pre defined functions for slip conditions were called into the solver and executed to update the near wall fluid velocity and temperature.

$$U_w - U_g = \left( \frac{2 - a_v}{a_v} \right) \frac{\lambda}{\delta} (U_g - U_c) \quad (7)$$

$$T_s - T_w = 2 \left( \frac{2 - a_T}{a_T} \right) \frac{\lambda}{\delta} (T_g - T_c) \quad (8)$$

$$\lambda = \frac{k_B T}{\sqrt{2\pi\sigma^2 p}} \quad (9)$$

At the beginning of simulation the driver and driven sections were patched with their corresponding pressures. A sudden rupture of diaphragm was assumed for the simulation. The domain was decomposed into structured quad elements with sufficient number of grid points for the numerical computation.

### Validation of Numerical Models

It is practically difficult to carry out experimental study for micro shock tubes of very small dimensions and at low pressure which was discussed in detail by the studies performed by Brouillette [3]. The greatest difficulty is in the availability of proper diaphragm material which will rupture at such low pressure. So in the present paper, due to the unavailability of any experimental data on this topic, every effort has been made to make a perfect numerical model. The numerical simulation results have a strong dependency on mesh quality and distribution. So to optimize the grid for reducing the numerical errors, a mesh independent study was carried out. For mesh independent study three different grids were considered for the simulation with same initial and boundary conditions. The final mesh (1500x25) which produced a lesser discrepancy in result compared to the previous cases, as shown in Fig.2, was chosen as the optimum mesh for further studies.

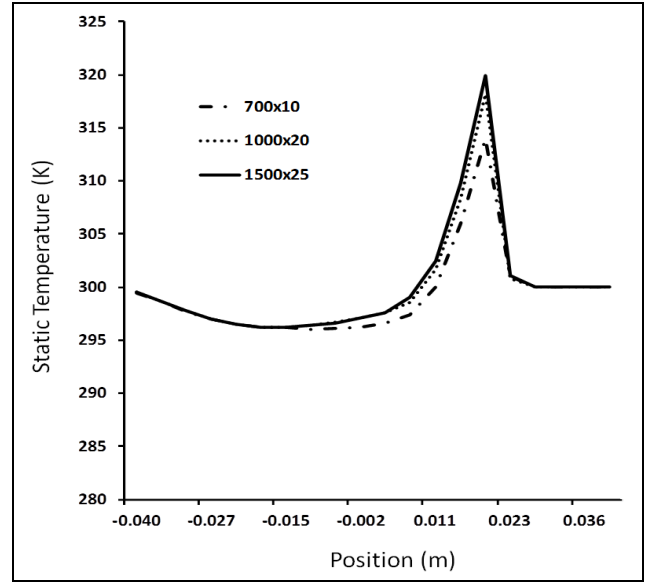


**Figure 2** Temperature distributions along axis (Case B) for different grids at  $t=5 \times 10^{-5}$  s

## TRENDS AND RESULTS

The investigation of shock movement inside a micro shock tube reveals that the shock front position lags from its ideal analytically determined locations. The analytical shock position was determined by multiplying the shock velocity with the corresponding time at which the shock location is needed to be computed. The shock velocity can be determined from the shock Mach number, which in turn can be determined from the invicid moving shock equation given below.

$$\frac{P_4}{P_1} = \frac{1 + \frac{2\gamma_1}{\gamma_1 + 1} (M_s^2 - 1)}{\left[ 1 - \frac{\gamma_4 - 1}{\gamma_4 + 1} \frac{a_1}{a_4} \left( M_s - \frac{1}{M_s} \right) \right]^{\frac{2\gamma_4}{\gamma_4 - 1}}} \quad (10)$$

The major drawback in evaluating the shock Mach number from the above equation is its invicid assumption. In fact this may not be the case for real situations. The shock movement induces the formation a thick boundary layer downstream of the shock front which can be noticed from Fig.3. This will produce strong viscous losses and yields to degradation in flow momentum.



**Figure 3** Axial velocity distribution (Case A) at  $t=1 \times 10^{-5}$  s

Owing to its small flow dimension, the shock propagation in a micro shock tube is heavily determined by the boundary layer and its associated losses which are negligible in the case of a macro shock tube. Another important parameter on which the shock speed depends is the initial pressure value existing in the tube sections. Even though ideal viscous shock equation, Eq.4, shows that the shock Mach number depends only on the pressure ratio and not on the initial pressure, this may not be accurate in the case of micro shock tube.

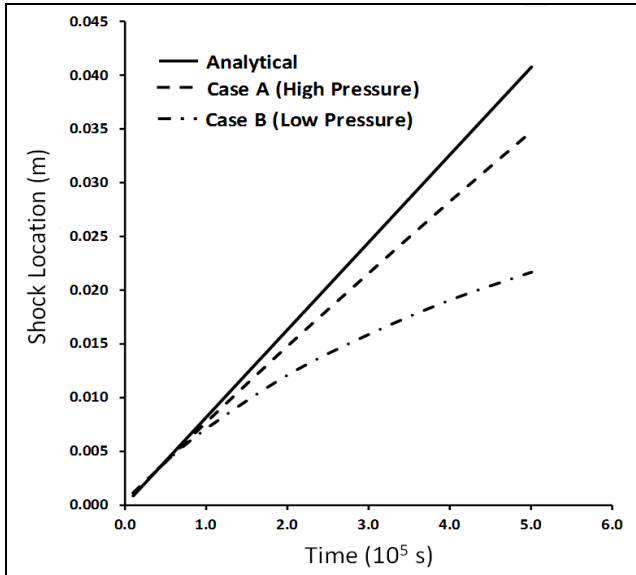


**Figure 4** Shock locations along axis ( $d=2\text{mm}$ ) at different initial pressure conditions

The simulation with lower pressure, Case B, shows that the shock speed diminishes with a reduction in pressure value, keeping the same pressure ratio. This can be clearly observed from Fig.4, showing the shock position for a 2mm diameter shock tube with same pressure ratios but different driver and driven section pressures. The reason for this effect can be attributed to the fact that as the pressure decreases the boundary layer thickness increases as shown in Fig.5. It is clear from the previous discussions that as the boundary layer thickness increases the flow losses will also get elevated leading to more attenuation of shock wave.

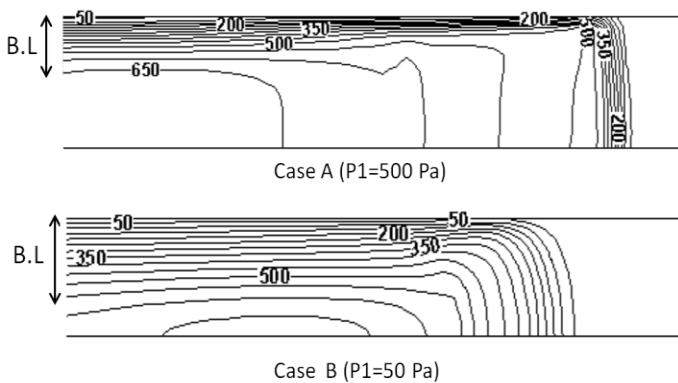


**Figure 5** Axial velocity distributions for Case A and Case B at  $t=1 \times 10^{-5}$  s

It is well known that as the pressure becomes very low rarefaction effects appears and the flow near the wall slips rather attaching to it. A jump in temperature can also be observed to the near wall fluid at these situations. The simulation with very low driven pressure, Case C, gives a Knudsen Number ( $Kn$ ) of 0.067 for the driven section. In general if the  $Kn$  is between 0.1 to 0.01, the flow exhibits rarefaction effects, which is included in the present case using Maxwell's equations.

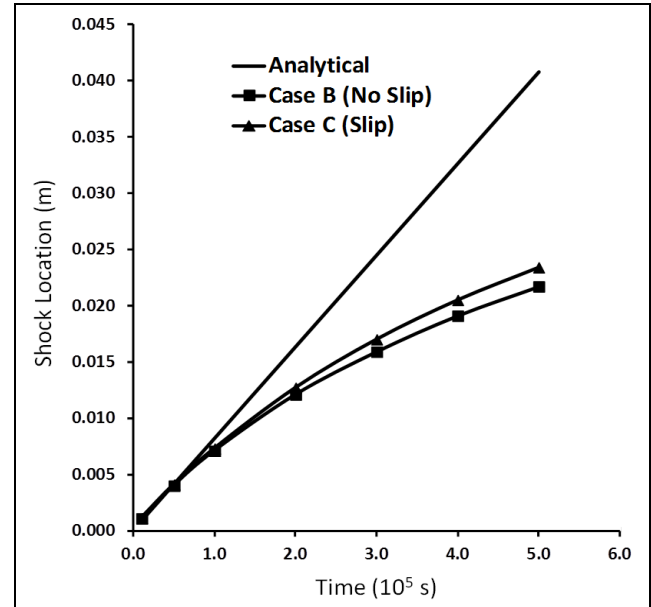


**Figure 6** Shock location along axis ( $d=2\text{mm}$ ) for slip and no slip case

With slip conditions the shock front moves faster compared to the no slip wall boundary. This effect is shown in Fig.6, indicating that the shock attenuation reduces under rarefied conditions.

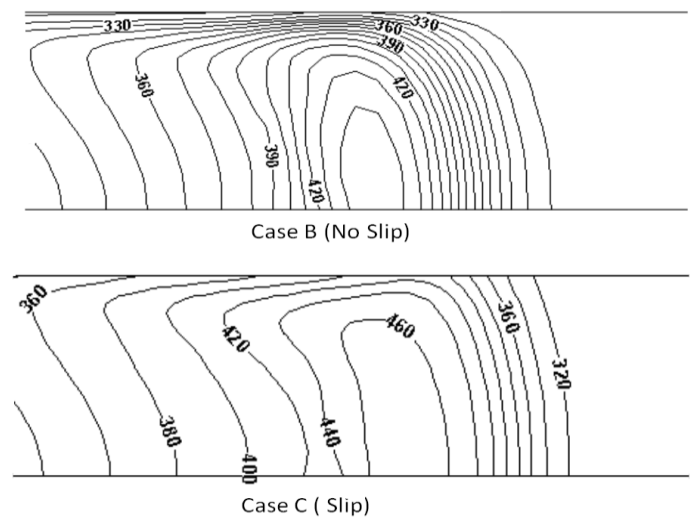


**Figure 7** Temperature distributions for no slip and slip cases ( $d=2\text{mm}$ ) at  $t=1 \times 10^{-5}$  s

The aid in shock propagation for slip case is due to the diminution in boundary layer effects caused by the non zero velocity and the temperature jump imparted to the near wall fluid. The wall losses will be diminished by these effects and the flow exhibits more core energy which in turn will reduce the attenuation. These effects can be visualised in Fig.7, which shows a comparison of temperature profile for slip and no slip case.

Fig.8 compares the shock position at various times for three different tube diameters (Case 1, 2 and 3 respectively).

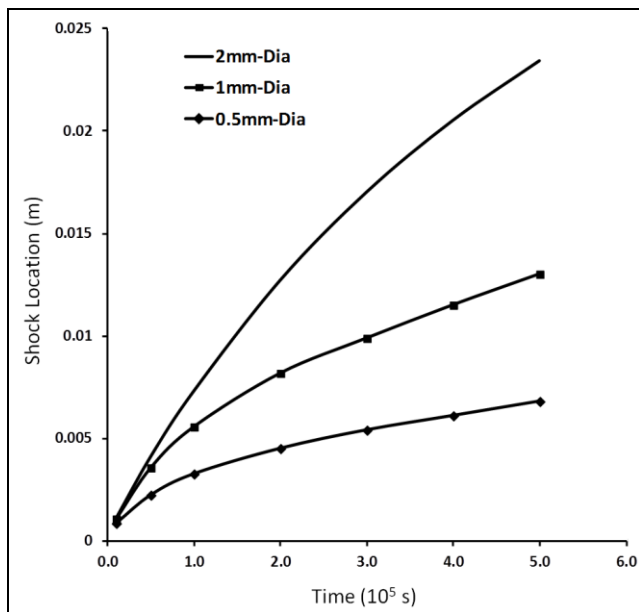


**Figure 8** Shock locations along axis for different tube diameters

It was observed that the shock strength drastically decreases with the reduction in diameter. As the tube diameter decreases, the boundary layer region takes up the majority of flow volume and the core flow will be narrowed. This leads to more losses in the shock strength and produce more attenuation.

The effect of reflected shock wave under slip and no slip conditions were compared for a 2mm shock tube. For this simulation the geometric length was changed with a 10 mm driver and 15 mm driven section. The initial and boundary conditions used were same as that of Case C. It is obvious that the reflected shock wave causes an increase in downstream pressure. This leads to an increase in Knudsen number behind the reflected shock front which makes the flow there to change back to no slip case. So the post reflected flow field obeys the same flow physics for both Slip and No Slip case and the shock wave diminishes into weak compression wave soon after reflection due to the additional losses. The reflected shock position comparison for slip and no slip cases are shown in Fig.9

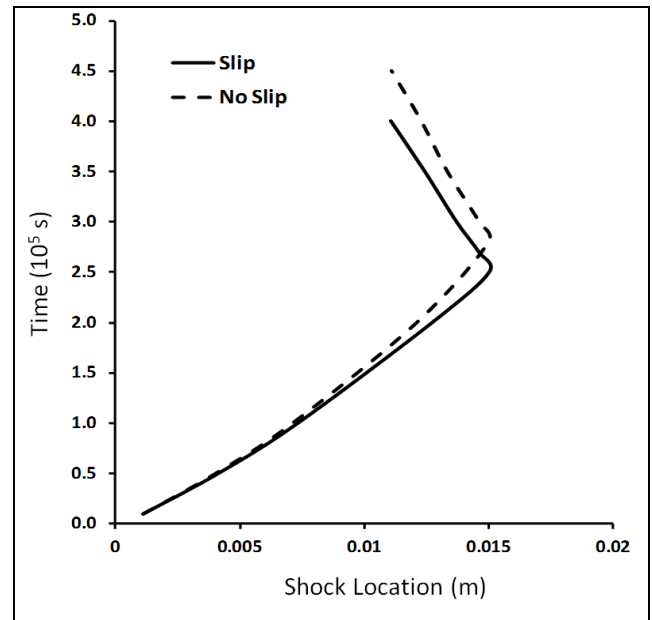


**Figure 9** Reflected shock locations along axis (d=2mm)

## CONCLUSION

Numerical simulations were carried out on micro shock tube to investigate shock wave propagation and reflection characteristics. Results show much more attenuation of shock strength for micro shock tube compared to macro shock tube. The attenuation effect can be attributed due to the viscous boundary layer formation which fills a considerable portion of the flow volume. The flow losses associated with this boundary layer degrades the core flow energy. As the driven section pressure reduces a thicker boundary layer forms compared to the high pressure case. This produces more loss in low pressure case and subsequently produces more attenuation to shock movement. The implementation of slip boundary condition on the walls to simulate the rarefaction effects reduces the losses produced by boundary layer. Thus rarefaction brings more preservation of core energy and causes less attenuation of shock wave compared to no slip case. The study of shock propagation on different tube diameter reveals that the shock attenuation increases drastically with reduction in diameter. This is because the boundary layer fills up a large portion of the core flow producing severe losses. When the shock reflects it increases the downstream pressure and if the initial pressure is not sufficiently low there is a huge possibility of the flow turning back again to no slip flow regime. This cause additional loss to the flow and the shock wave get transformed into weak compression wave soon after reflection.

## ACKNOWLEDGEMENT

This work was supported by the National Research Foundation of Korea (NRF) grant funded by the Korea government (MEST) (2011-0017506).

## REFERENCES

- [1] Duff, R.E., Shock tube performance at initial low pressure, *Phys. Fluids*, Vol.2, 1959, pp. 207-216
- [2] Mirels, H., Test time in low pressure shock tube, *Phys. Fluids*, Vol. 6, 1963, pp. 1201-1214
- [3] Brouillette, M., Shock waves at microscales, *Shock Waves*, Vol. 13, 2003, pp.03-012
- [4] Zeitoun, D. E., Burtschell, Y., Navier- Stokes computations in micro shock tubes, *Shock Waves*, vol. 15, 2006, pp. 241-246
- [5] Zeitoun, D. E., Burtschell, Y., Graur, I. A., Ivanov, M. S., Kudryavtsev, A. N., Bondar, Y. A., Numerical simulation of shock wave propagation in micro channels using continuum and kinetic approaches, *Shock Waves*, Vol. 19, 2009, pp. 307-316
- [6] Fichman, M., Hetsroni, G., Viscosity and slip velocity in gas flow in microchannels, *Phys. Fluids*, Vol. 17, 2005, pp. 1201-1214
- [7] Amit Agrawal., Lyazid Djenidi ., Antonia, R.A., Simulation of gas flow in microchannels with a sudden expansion or contraction, *Journal of Fluid Mechanics*, Vol. 530, 2005, pp. 135-144
- [8] Giulio Croce., Paola D'Agaro., Numerical analysis of roughness effect on microtube heat transfer, *Superlattices and Microstructures*, Vol. 35, 2004, pp. 601-616
- [9] Karniadakis, G. E. M., Beskok, A., *Micro Flows fundamentals and Simulation*, Springer, Berlin Heidelberg, New York, 2000.
- [10] Fluent user's guide manual, <http://www.fluent.com/>